Comput Mech (2012) 49:477–485
DOI 10.1007/s00466-011-0656-8

ORIGINAL PAPER

Shakedown analysis with multidimensional loading spaces

Jaan-Willem Simon · Dieter Weichert

Received: 9 August 2010 / Accepted: 20 October 2011 / Published online: 3 November 2011

Abstract A numerical method for the computation of shakedown loads of structures subjected to varying thermal and mechanical loading is proposed for the case of multidimensional loading spaces. The shakedown loading factors are determined based on the lower bound direct method using the von Mises yield criterion. The resulting nonlinear convex optimization problem is solved by use of the interior-point method. Although the underlying theory allows for the consideration of arbitrary numbers of loadings in principle, until now applications have been restricted to special cases, where either one or two loads vary independently. In this article, former formulations of the optimization problem are generalized for the case of arbitrary numbers of loadings. The method is implemented into an interior-point algorithm specially designed for this method. For illustration, numerical results are presented for a three-dimensional loading space applied to a square plate with a central circular hole.

Keywords Direct method · Shakedown analysis · Interior-point algorithm · Large-scale problem · Multidimensional loading space

1 Introduction

For the design of engineering structures it is most important to reliably predict whether or not the considered system is capable of resisting to the given loading beyond the elastic limit. Different failure mechanisms can occur, in particular if the loads vary as function of time. In case of instantaneous collapse, the system fails during the first loading cycle, whereas the accumulation of plastic strains from several loading cycles can lead to incremental collapse (ratcheting). However, plastic deformations may eventually lead to failure even if the amount of total plastic deformation is limited and remains small, but the plastic strain increments occur in an alternating manner, which is often referred to as alternating plasticity. If none of these failure mechanisms occurs, one says that the system shakes down.

The according shakedown load can be determined most conveniently by using direct methods [1–3]. These will be applied in this study using the lower bound shakedown theorem by Melan [4,5]. Their most appreciable advantage is the fact that the loading history does not need to be given deterministically, but only its bounding envelope [6]. However, direct methods lead to nonlinear convex optimization problems. For engineering problems of practical relevance, this generally implies large numbers of variables and constraints.

Direct methods have been handicapped for long time by the lack of appropriate tools in nonlinear optimization. However, the substantial increase in computational capabilities in recent years allowed for the development of efficient numerical methods in this field. Among the existing approaches for the solution of nonlinear optimization problems, we focus on the *interior-point method* [7–11], which has been implemented into several software packages for general nonlinear programming, such as LOQO [12,13], KNITRO [14,15] and IPOPT [16–18].

These codes are quite powerful, as shown, e.g., in the comparative studies [19,20], and cover a wide range of applications. Nevertheless, they often lack efficiency compared to specialized algorithms in case of large numbers of variables and constraints. Therefore, they have hardly been applied in the context of direct methods, as e.g., IPOPT in [21] and [22]. To overcome this problem, following [23], second order cone programming (SOCP) has been widely used in recent years, in

J.-W. Simon (✉) · D. Weichert
Institute of General Mechanics, RWTH Aachen University,
Templergraben 64, 52056 Aachen, Germany
e-mail: jaan.simon@rwth-aachen.de

particular, the software package MOSEK [24] e.g., in [25–29], as well as the codes SEDUMI [30] and SDPT3 [31] in [32].

Another possibility to improve the numerical procedures focuses on the prior structural analysis. For example, instead of the standard finite element method (FEM), in [33] the symmetric Galerkin boundary element method (BEM) has been used, whereas in [34] the meshless element-free Galerkin method (EFG) has been introduced to the solution procedure. Non-standard FEM has been applied, e.g., in [35,36] for cell-based smoothed elements (CS- FEM) and for edge-based smoothed elements (ES- FEM), respectively. In [37] a non-conforming element is proposed, which is constructed from bilinear shape functions and enriched by internal second-order polynomials. Furthermore, alternative methodologies have been published in [38,39] on the basis of piece-wise linearization of the yield surface and in [40] where a strain-driven strategy is proposed.

Nevertheless, the use of appropriate numerical tools to solve nonlinear optimization problems is of crucial relevance in the field of direct methods. Since not all kinds of problems in limit and shakedown analysis can be formulated as SOCP and for better computational performance through problem-tailored solution procedures, some independent interior-point algorithms have been presented for both limit analysis, e.g., [41–45], and shakedown analysis, e.g., [46–51].

Based on previous work [52,53] on the DC- decomposition, in [48–50] the interior-point algorithm IPDCA has been presented and successfully applied to problems of shakedown analysis with either one or two independently varying loads. On the basis of IPDCA, a new interior-point algorithm has been proposed recently in [54–56], which is characterized by a problem-oriented solution strategy for the specific case of von Mises materials. Moreover, several numerical advancements in the new algorithm lead to a more stable performance.

In this article, a new formulation is presented, that allows for the computation of shakedown loading factors for arbitrary numbers of thermal and mechanical loadings. The described methodology is illustrated by application to a square plate with a central circular hole subjected to three independent loadings. To our knowledge, no results on shakedown analysis with more than two independently varying loadings have been obtained before.

2 Static approach of shakedown analysis

We use the statical shakedown theorem by Melan [4,5] to determine the shakedown factor α_{SD}, which is the maximum loading factor α such that the system does not fail due to incremental collapse or alternating plasticity. Here, we restrict ourselves to elastic-perfectly plastic, time-independent material behavior. Furthermore, geometrical nonlinearity is not considered. In addition, we assume the existence of a convex yield function $F\left(\boldsymbol{\sigma}(\boldsymbol{x},t),\sigma_Y(\boldsymbol{x})\right)$ such that the normality rule is satisfied, where $\sigma_Y(\boldsymbol{x})$ denotes the yield stress in the point $\boldsymbol{x}$.

Then, Melan's theorem states that the system will shake down if one can find a loading factor $\alpha > 0$ and a time-independent residual stress field $\bar{\boldsymbol{\rho}}(\boldsymbol{x})$ whose superposition with the purely elastic stress field $\boldsymbol{\sigma}^E(\boldsymbol{x},t)$ satisfies the yield condition at any time t in any point $\boldsymbol{x}$ of the structure.

$$\forall \boldsymbol{x},\ \forall t: \quad F\left(\alpha\,\boldsymbol{\sigma}^E(\boldsymbol{x},t)+\bar{\boldsymbol{\rho}}(\boldsymbol{x}),\sigma_Y(\boldsymbol{x})\right)\le 0 \tag{1}$$

For the application, the total stresses $\boldsymbol{\sigma}$ are decomposed into two parts, $\boldsymbol{\sigma} = \boldsymbol{\sigma}^E + \bar{\boldsymbol{\rho}}$. The residual stress field $\bar{\boldsymbol{\rho}}$ is induced by the evolution of plastic deformation, whereas $\boldsymbol{\sigma}^E$ denotes the elastic stress field which would occur in a purely elastic reference body under the same conditions and loading. Since the elastic reference stress field $\boldsymbol{\sigma}^E$ is in equilibrium with the external loading, the residual stress field $\bar{\boldsymbol{\rho}}$ is self-equilibrated and the principle of virtual work reads as follows, [57].

$$\int_V \delta\boldsymbol{\varepsilon} : \bar{\boldsymbol{\rho}}\, dV = 0 \tag{2}$$

Here, $\delta\boldsymbol{\varepsilon}$ denotes a virtual strain field, which satisfies the kinematical boundary conditions. Using the FEM, this virtual strain field is approximated based on appropriate shape functions for the displacements using the relation $\boldsymbol{\varepsilon} = \frac{1}{2}(\boldsymbol{\nabla u} + \boldsymbol{u\nabla})$. Carrying out the integration numerically, Eq. 2 is thereby converted into a system of linear equations for the residual stresses $\bar{\boldsymbol{\rho}}_r$ evaluated in the Gaussian points $r \in [1, NG]$, where NG denotes the total number of Gaussian points of the system.

$$\sum_{r=1}^{NG} \mathbb{C}_r \cdot \bar{\boldsymbol{\rho}}_r = \mathbf{0} \tag{3}$$

The so-called equilibrium matrices $\mathbb{C}_r \in \mathbb{R}^{m_E \times 6}$ only depend on the geometry of the system and the chosen element type. They can be calculated using the principle of virtual work and are computed by the user-defined subroutine UEL in ANSYS. Their dimension is $m_E = 3\,NK - NBC$, where NK is the total number of nodes and NBC is the number of kinematical boundary conditions.

With (1) and (3) the shakedown loading factor α_{SD} can be computed from the following optimization problem on the basis of Melan's theorem.

$$(\mathcal{P}_M) \qquad \alpha_{SD} = \max \alpha$$
$$\sum_{r=1}^{NG} \mathbb{C}_r \cdot \bar{\boldsymbol{\rho}}_r = \mathbf{0} \tag{4a}$$

$$\forall r \in [1, NG]\,,\ \forall t\ :$$
$$F\left(\alpha\,\boldsymbol{\sigma}_r^E(t) + \bar{\boldsymbol{\rho}}_r\,,\ \sigma_{Y,r}\right) \le 0 \tag{4b}$$

3 Description of the loading domain in multidimensional loading spaces

The considered structure is subjected to an arbitrary finite number NL of loads P_ℓ. Thus, we restrict ourselves to loading histories $\mathcal{H}(\boldsymbol{x}, t)$ which can be expressed as combinations of the NL loading cases, where the time-dependency is captured through the introduction of loading multipliers $\mu_\ell(t)$ for each loading case. Here, we scale all loads to the generalized unity load P_0.

$$\mathcal{H}(\boldsymbol{x}, t) = \sum_{\ell=1}^{NL} P_\ell(\boldsymbol{x}, t) = \sum_{\ell=1}^{NL} \mu_\ell(t)\, P_0(\boldsymbol{x}) \tag{5}$$

As shown in [6], it is sufficient to only consider the bounding envelope of the loading history. Therefore, the bounds of each of the loading multipliers are defined.

$$\mu_\ell^- \le \mu_\ell(t) \le \mu_\ell^+ \tag{6}$$

Merging the load multipliers into the vector $\boldsymbol{\mu} = \mu_\ell\, \boldsymbol{e}_\ell$, the set $\mathcal{K}$ of all possible combinations of loading cases within these bounds can be defined as follows.

$$\mathcal{K} = \left\{ \boldsymbol{\mu} \in \mathbb{R}^{NL} \middle| \mu_\ell^- \le \mu_\ell \le \mu_\ell^+\,,\ \forall \ell \in [1, NL] \right\} \tag{7}$$

Then, the loading domain Ω can be defined as set of all possible loading histories within the bounding envelope described by (7).

$$\Omega = \left\{ \mathcal{H}(\boldsymbol{x}, t) \middle| \mathcal{H}(\boldsymbol{x}, t) = \sum_{\ell=1}^{NL} \mu_\ell(t)\, P_0(\boldsymbol{x})\,,\ \forall \boldsymbol{\mu} \in \mathcal{K} \right\} \tag{8}$$

In analogy to (5), the elastic reference stresses are decomposed according to the loading cases.

$$\boldsymbol{\sigma}^E(\boldsymbol{x}, t) = \sum_{\ell=1}^{NL} \mu_\ell(t)\, \boldsymbol{\sigma}_\ell^E(\boldsymbol{x}) \tag{9}$$

As before, using the FEM allows for the formulation of the stresses in terms of the values in the Gaussian points $r \in [1, NG]$. The stresses $\boldsymbol{\sigma}_{r,\ell}^E$ can be computed as result of purely elastic analysis for the loading case ℓ with standard FEM software.

$$\boldsymbol{\sigma}_r^E(t) = \sum_{\ell=1}^{NL} \mu_\ell(t)\, \boldsymbol{\sigma}_{r,\ell}^E \tag{10}$$

The NL given loads span an NL-dimensional polynomial loading domain Ω with $NC = 2^{NL}$ corners. Since it is sufficient to consider only the corners of the loading domain, the time-dependence of $\boldsymbol{\sigma}^E$ can be expressed through the stress states in these corners $j \in [1, NC]$. This is done by introducing the matrix $\boldsymbol{U}_{NL} \in \mathbb{R}^{NC \times NL}$ with entries $U_{j\ell}$, where $j \in [1, NC]$ and $\ell \in [1, NL]$.

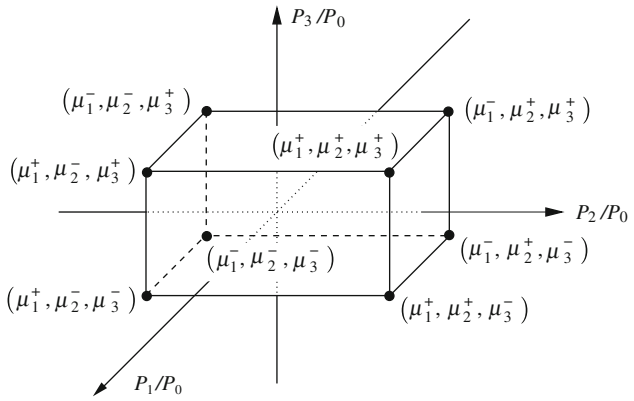

Fig. 1 Loading domain in a three-dimensional loading space

$$\boldsymbol{\sigma}_r^{E,j} = \sum_{\ell=1}^{NL} U_{j\ell} \boldsymbol{\sigma}_{r,\ell}^E \tag{11}$$

Each row of the matrices $\boldsymbol{U}_{NL}$ represents the coordinates of one corner of the loading domain in the NL-dimensional loading space – scaled with the load P_0. Thus, the introduction of $\boldsymbol{U}_{NL}$ requires the definition of the corners of the loading domain with the given factors μ_i^- and μ_i^+ as introduced in (6). In order to define such a matrix $\boldsymbol{U}_{NL}$ for arbitrary numbers of loading cases NL, the corners of the loading domain are arranged in a specific order. For illustration, we begin with the case of three independent loads, $NL = 3$. The according domain in the three-dimensional loading space is illustrated in Fig. 1 with the associated matrix $\boldsymbol{U}_3$ (12).

$$\boldsymbol{U}_3 = \begin{bmatrix} \mu_1^+ & \mu_2^+ & \mu_3^+ \\ \mu_1^- & \mu_2^+ & \mu_3^+ \\ \hline \mu_1^+ & \mu_2^- & \mu_3^+ \\ \mu_1^- & \mu_2^- & \mu_3^+ \\ \hline \mu_1^+ & \mu_2^+ & \mu_3^- \\ \mu_1^- & \mu_2^+ & \mu_3^- \\ \hline \mu_1^+ & \mu_2^- & \mu_3^- \\ \mu_1^- & \mu_2^- & \mu_3^- \end{bmatrix} \tag{12}$$

The third column consists of two divisions of length 4, where μ_3^+ is the value of all entries in the first part, and in the second part all entries have the value μ_3^-. We denote such a substructure by *block*. Then, the second column can be divided into two blocks having two entries μ_2^+ and μ_2^- each, whereas the first column comprises four blocks with one entry μ_1^+ and μ_1^- each. This ordering scheme can be generalized for the case of arbitrary finite numbers of loadings NL. The last column of the associated matrix $\boldsymbol{U}_{NL} \in \mathbb{R}^{NC \times NL}$ consists of one block with $NC/2$ entries μ_{NL}^+ and

μ_{NL}^{-}. The penultimate column is composed of two blocks with $NC/4$ entries μ_{NL-1}^{+} and μ_{NL-1}^{-}, and so on. Finally, the first column can be divided into $NC/2$ blocks, where each of the blocks consists of one pair μ_1^{+} and μ_1^{-} only.

Thereby, the matrices $\boldsymbol{U}_{NL} \in \mathbb{R}^{NC\times NL}$ can be constructed column-wise in the following way:

For $l = 1, 2, \ldots, NL$ do the following:
in the considered column l write 2^{NL-l} blocks one below the other, where each block consists of 2^{l-1} entries with the maximum value μ_l^{+} followed by 2^{l-1} entries with the minimum value μ_l^{-}

4 Solution procedure with interior-point method

The yield condition (1) has to be satisfied for all Gaussian points $r \in [1, NG]$ and all corners of the loading domain $j \in [1, NC]$.

$$\forall r \in [1, NG]\ ,\ \forall j \in [1, NC]: \\ F\left(\alpha\, \boldsymbol{\sigma}_r^{E,j} + \bar{\boldsymbol{\rho}}_r\ ;\ \sigma_{Y,r}\right) \le 0$$

The solution procedure of the presented algorithm IPSA is specially tailored to the von Mises yield criterion, which leads to significant benefits in the performance compared to general solvers. The necessary transformations and implementation issues are described in [56] and will not be repeated here. However, the resulting optimization problem $(\mathcal{P}_{IP})$ reads as follows.

$$(\mathcal{P}_{IP}) \qquad \min f(\boldsymbol{x}) = -\alpha$$
$$\boldsymbol{A}\cdot\boldsymbol{x} = \boldsymbol{0} \tag{13a}$$
$$\boldsymbol{c}_I(\boldsymbol{x}) \ge \boldsymbol{0} \tag{13b}$$
$$\boldsymbol{x} \in \mathbb{R}^n \tag{13c}$$

The problem consists of $m_E^* = m_E + 5NG\cdot(NC-1)$ equality constraints (13a), $m_I = NG\cdot NC$ inequality constraints (13b) and $n = (5NC+1)\cdot NG+1$ variables, which are merged in the solution vector $\boldsymbol{x}$. The objective function $f(\boldsymbol{x})$ is linear, the equality constraints are affine-linear with the constant coefficient matrix $\boldsymbol{A} \in \mathbb{R}^{m_E^*\times n}$ and the inequality constraints are nonlinear and concave. Moreover, the Slater condition is satisfied by definition. Thus, the optimization problem is regular, nonlinear and convex.

The solution of this problem is obtained by application of the interior-point method. Slack variables $\boldsymbol{w}$ are introduced to transform the inequality constraints into equality constraints. In addition, split variables $\boldsymbol{y}$ and $\boldsymbol{z}$ are inserted into (13c) to handle the free variable $\boldsymbol{x}$, because otherwise its unboundedness might lead to numerical instabilities, see e.g., [58].

Then, to ensure that the solution of the problem cannot leave the feasible region described by the subsidiary conditions, barrier terms are added to the objective function. Here, we use logarithmic barriers weighted by a barrier parameter μ which tends to zero during the iteration.

$$f_\mu(\boldsymbol{x},\boldsymbol{y},\boldsymbol{z},\boldsymbol{w}) = f(\boldsymbol{x}) - \mu\left[\sum_{i=1}^{n}\log(y_i) + \sum_{i=1}^{n}\log(z_i) + \sum_{j=1}^{m_I}\log(w_j)\right] \tag{14}$$

The resulting problem thus takes the form:

$$(\mathcal{P}_\mu) \quad \min f_\mu(\boldsymbol{x},\boldsymbol{y},\boldsymbol{z},\boldsymbol{w})$$
$$\boldsymbol{A}\cdot\boldsymbol{x} = \boldsymbol{0} \tag{15a}$$
$$\boldsymbol{c}_I(\boldsymbol{x}) - \boldsymbol{w} = \boldsymbol{0} \tag{15b}$$
$$\boldsymbol{x} - \boldsymbol{y} + \boldsymbol{z} = \boldsymbol{0} \tag{15c}$$
$$\boldsymbol{w} > \boldsymbol{0},\ \boldsymbol{y} > \boldsymbol{0},\ \boldsymbol{z} > \boldsymbol{0} \tag{15d}$$

with the Lagrangian of $(\mathcal{P}_\mu)$:

$$\mathcal{L} = f_\mu(\boldsymbol{x},\boldsymbol{y},\boldsymbol{z},\boldsymbol{w}) - \boldsymbol{s}\cdot(\boldsymbol{x}-\boldsymbol{y}+\boldsymbol{z}) - \boldsymbol{\lambda}_E\cdot(\boldsymbol{A}\cdot\boldsymbol{x}) - \boldsymbol{\lambda}_I\cdot(\boldsymbol{c}_I(\boldsymbol{x})-\boldsymbol{w})\,, \tag{16}$$

where $\boldsymbol{\lambda}_E \in \mathbb{R}^{m_E^*}$, $\boldsymbol{\lambda}_I \in \mathbb{R}_+^{m_I}$ and $\boldsymbol{s} \in \mathbb{R}_+^n$ are Lagrange multipliers. This function can be used to apply the Karush–Kuhn–Tucker conditions (KKT) which are necessary and sufficient optimality conditions for regular convex problems [59]. The KKT state that a solution is optimal if and only if the Lagrangian $\mathcal{L}$ possesses a saddle point,

$$\boldsymbol{\nabla}_{\Pi}\mathcal{L} = \boldsymbol{0}, \tag{17}$$

where $\boldsymbol{\nabla}_{\Pi}(.)$ denotes the gradient in all variables $\boldsymbol{\Pi}$ of the problem. The system of nonlinear equations (17) is solved by use of the Newton method. The step values $\Delta\boldsymbol{\Pi}_k$ in the iteration step $k+1$ are computed from the known values $\boldsymbol{\Pi}_k$ of the previous iteration step k.

$$\boldsymbol{J}(\boldsymbol{\Pi}_k)\cdot\Delta\boldsymbol{\Pi}_k = -\boldsymbol{\nabla}_{\Pi}\mathcal{L}(\boldsymbol{\Pi}_k) \tag{18}$$
$$\text{where: } \boldsymbol{J}(\boldsymbol{\Pi}_k) = \boldsymbol{\nabla}_{\Pi}\mathcal{L}(\boldsymbol{\Pi})\,\boldsymbol{\nabla}_{\Pi}\Big|_{\boldsymbol{\Pi}=\boldsymbol{\Pi}_k}$$

Note, that general solvers typically use the complete Jacobian for the solution of (18), whereas we take advantage of the specific structure of the involved matrices to reduce the system by appropriate substitution of variables, which significantly reduces the running time (see also [56]).

Once the step values $\Delta\boldsymbol{\Pi}_k$ have been calculated as the solution of the system of linear equations (18), the variables $\boldsymbol{\Pi}_{k+1}$ of the subsequent step $k+1$ can be determined by (19).

$$\boldsymbol{\Pi}_{k+1} = \boldsymbol{\Pi}_k + \boldsymbol{\Upsilon}_k\cdot\Delta\boldsymbol{\Pi}_k \tag{19}$$

Here, the diagonal matrix $\boldsymbol{\Upsilon}_k$ of damping factors ensures the non-negativity conditions of slack and split variables and Lagrange multipliers. In addition, damping of the Newton step can guarantee that the computed step is associated with

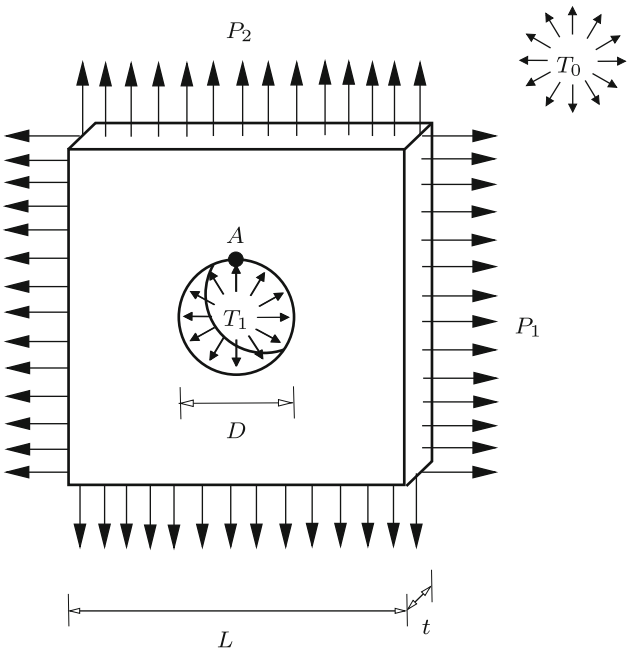

Fig. 2 System and loading cases

Table 1 Dimensions of the plate

Length L in (mm)	100
Thickness t in (mm)	2
Diameter D in (mm)	20

Table 2 Thermal and mechanical characteristics

Young's modulus (MPa)	7.24×10^4
Yield stress (MPa)	345
Poisson's ratio	0.33
Density (kg/m^3)	2.78×10^3
Thermal conductivity (W/(m^2 K))	151
Specific heat capacity (J/(kg K))	875
Coefficient of thermal expansion	2.47×10^{-5}
Transfer coefficient at boundary (W/(m^2 K))	200
Transfer coefficient in hole (W/(m^2 K))	1200

a descent direction. For this, we apply a linesearch strategy using an ℓ_2-merit function, if necessary [56].

5 Numerical example

The described algorithm is applied to a square plate with a circular hole. The considered system is illustrated in Fig. 2.

The characteristic dimensions are given in Table 1.

The plate is made of 2024–T6 aluminum and is assumed to be homogeneous and isotropic. The thermal and mechanical characteristics are given in Table 2.

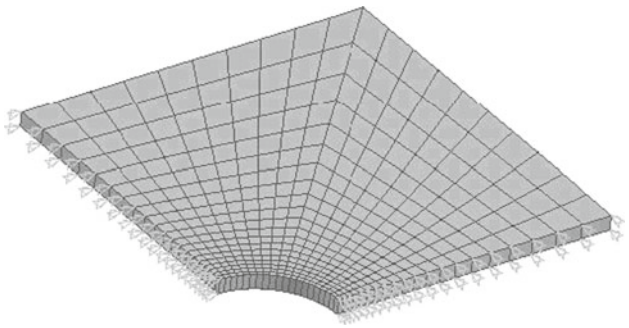

Fig. 3 FEM-model and mesh

All material parameters are assumed to be independent of the applied temperature. The loading process is considered to be quasi-static. No transient thermal effects are taken into account. Creep due to the high temperature is not included in the current calculation.

Due to the symmetry of the system, only one quarter of the plate is considered with according boundary conditions. The system is discretized by isoparametric, hexahedral elements in ANSYS. For the thermal analysis the element-type *solid70* and for the structural analysis the element-type *solid185* have been used. The mesh consists of 882 nodes and 400 elements and is shown in Fig. 3.

Two different types of loading will be considered separately:

1. The two-dimensional case is a typical benchmark problem for validation of algorithms for shakedown analysis. Two uniform normal tractions P_1 and P_2 are applied which vary independently of each other.
2. In the three-dimensional case the plate is additionally subjected to a thermal loading ΔT which is applied on the boundary of the hole. All three loads vary independently of each other.

5.1 Two-dimensional loading space

In the two-dimensional case, the plate is subjected to two uniform normal tractions P_1 and P_2 which are applied in both directions perpendicular to the sides of the square. For the calculation of the elastic stresses an arbitrary value $P_0 = 100$ MPa has been used. The two loads vary in the following ranges:

$$0 \le P_1 \le \mu_1^+ P_0 \tag{20a}$$

$$0 \le P_2 \le \mu_2^+ P_0 \tag{20b}$$

The larger one of μ_1^+ and μ_2^+ is normalized to one. The associated two-dimensional loading domain is illustrated in Fig. 4.

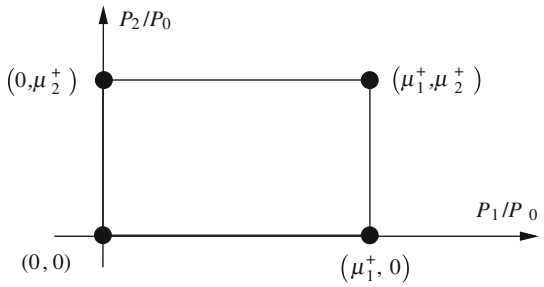

Fig. 4 Loading domain in the two-dimensional calculation

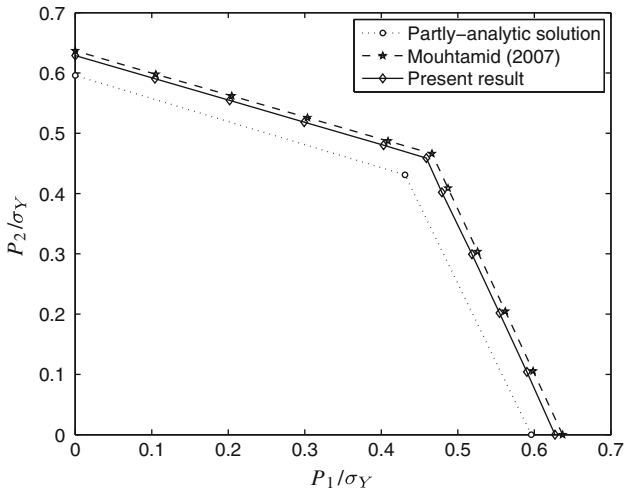

Fig. 5 Shakedown domain in 2D-case without temperature

Results for this problem have been presented by many authors, e.g., [36,60–71]. Comparative studies of these and other works have been given in [33,46,57,72]. The comparison with most of these has been presented in [56]. We avoid repetition and confine ourselves to compare our results exemplarily to the ones obtained by Mouhtamid [70] and to the partly-analytical solution in [73] (Fig. 5).

5.2 Three-dimensional loading space

In the three-dimensional case, a thermal load ΔT is applied to the boundary of the hole in addition to the two normal tractions P_1 and P_2. For the calculation of the elastic stresses the arbitrary values $P_0 = 100$ MPa, $T_1 = 500$ K and $T_0 = 300$ K have been used. We choose $\mu_1^- = \mu_2^- = \mu_3^- = 0$ such that the loads vary independently in the following ranges:

$$0 \leq P_1 \leq \mu_1^+ P_0 \tag{21a}$$

$$0 \leq P_2 \leq \mu_2^+ P_0 \tag{21b}$$

$$0 \leq \Delta T \leq \mu_3^+ \Delta T_0 \tag{21c}$$

The loading domain is given in Fig. 6. Moreover, the 111 points in the three-dimensional loading space are shown, for

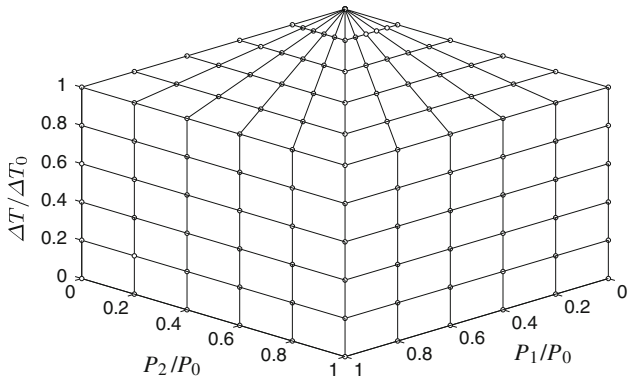

Fig. 6 Computed points in loading space

which the calculation of the shakedown factor has been carried out.

The results can be presented as a sequence of two-dimensional plots as shown in Fig. 7. Here, the solutions for different fixed ratios μ_1^+/μ_2^+ are illustrated, each of them representing a fixed angle in the P_1-P_2–plane. Note, that only the ratio of the maximum factors is kept constant in these cases, whereas all three loads vary independently in all calculations.

In Fig. 8 the three-dimensional shakedown domain is shown. For the purpose of a clear presentation, the point (0, 0, 22.823) is not plotted. Otherwise, the distance between the plotted points would have to be reduced. The numerical results for some specific ratios are given in Table 3. In order to get a material-independent presentation, the coordinates of the points are given in the scaled loading space.

In Table 4 numerical details for the two-dimensional and the three-dimensional case are compared. For both cases, the relevant numbers describing the problem's dimension are presented as well as the mean values of the number of iterations and the CPU-time. The latter ones are used to demonstrate a tendency and shall not be used for an exact comparison, because the average is taken over a different total number of values.

Since the number of iterations is very sensitive to the applied convergence criteria and tolerances, the absolute value may not be as important as the comparison between the different cases. Thus, the number of iterations is scaled to the one in the two-dimensional case. The same holds for the given value of CPU-time due to the sensitivity to the used computer.

5.3 Discussion of results

The high values of the computed shakedown factors in the case that the temperature load predominates the normal tractions, $\mu_1^+ < 0.5\,\mu_3^+$ and $\mu_2^+ < 0.5\,\mu_3^+$, are only of theoretical interest, because the assumption of temperature- independence of the material parameters is no more valid due to

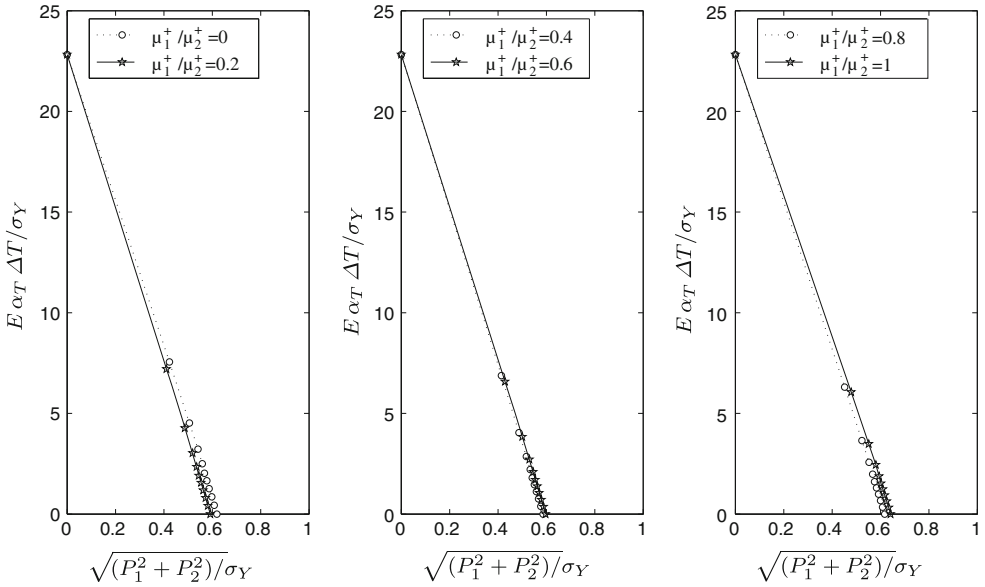

Fig. 7 Shakedown domains in planes for fixed ratios μ_1^+/μ_2^+

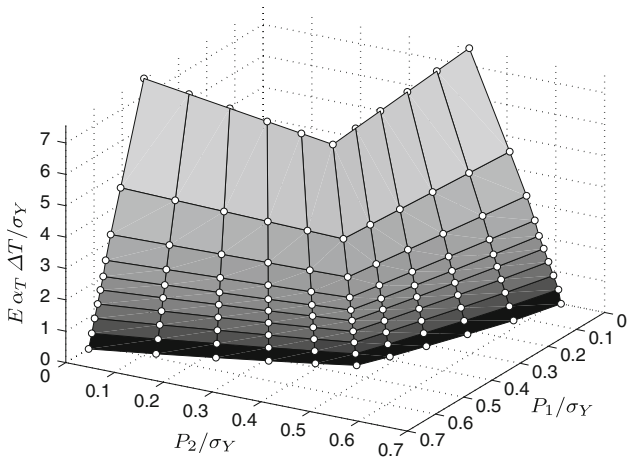

Fig. 8 Shakedown domain in three-dimensional loading space

the high temperatures. Nevertheless, as expected, also in the range of predominating normal tractions, there is an important influence of the temperature loading on the shakedown factor.

The number of variables in the three-dimensional case is nearly twice the number in the two-dimensional case, as can be seen in Table 4. The number of constraints is even more than doubled. Thus, the significant increase of running time is not astonishing. However, the small difference in the number of iterations is remarkable.

6 Conclusions

A new method for the application of shakedown analysis to the case of multidimensional loading spaces has been presented, allowing to compute shakedown domains of structures subjected to arbitrary finite numbers of independent thermo-mechanical loads.

Table 3 Numerical results of shakedown analysis in three-dimensional loading space

$(\mu_1^+, \mu_2^+, \mu_3^+)$	P_1/σ_Y	P_2/σ_Y	$E\,\alpha_T\,\Delta T/\sigma_Y$
(1, 0, 0)	0.619	0	0
(0, 1, 0)	0	0.611	0
(0, 0, 1)	0	0	22.823
(1, 1, 0)	0.454	0.454	0
(0, 1, 1)	0	0.566	2.022
(1, 0, 1)	0.568	0	2.029
(1, 1, 1)	0.426	0.426	1.523
(0.5, 0.5, 1)	0.402	0.402	2.876
(0.5, 1, 0.5)	0.254	0.508	0.908
(1, 0.5, 0.5)	0.508	0.254	0.907
(0.5, 1, 1)	0.244	0.489	1.748
(1, 0.5, 1)	0.489	0.244	1.747
(1, 1, 0, 5)	0.440	0.440	0.786

Table 4 Comparison between the 2D- and 3D-computation

	2D-case	3D-case
NK	882	882
NG	3200	3200
NC	4	8
n	67201	131201
m_E^*	50646	114646
m_I	12800	25600
∅ No. of iter. (%)	100	113
∅ CPU-time (%)	100	249

The algorithm has been used for the computation of the shakedown loading factors of a plate subjected to three thermo-mechanical loads which vary independently of each other. The associated three-dimensional loading space and the three-dimensional shakedown domain have been presented.

References

1. Weichert D, Maier G (2000) Inelastic analysis of structures under variable repeated loads. Kluwer Academic Publishers, Dordrecht
2. Maier G, Pastor J, Ponter ARS, Weichert D (2003) Direct methods of limit and shakedown analysis. In: de Borst R, Mang HA (eds) Comprehensive structural integrity: fracture of materials from nano to macro, volume 3: Numerical and computational methods. Elsevier, Amsterdam, pp 637–684
3. Weichert D, Ponter ARS (2009) Limit states of materials and structures. Springer, Wien/New York
4. Melan E (1938) Zur Plastizität des räumlichen Kontinuums. Ing-Arch 9:116–126
5. Melan E (1938) Der Spannungszustand eines "Mises-Hencky'schen" Kontinuums bei veränderlicher Belastung. Sitzungsberichte/Akademie der Wissenschaften in Wien, Mathematisch-Naturwissenschaftliche Klasse Abteilung IIa, 147:73–87
6. König JA (1987) Shakedown of elastic-plastic structures. Elsevier, Amsterdam
7. El-Bakry AS, Tapia RA, Tsuchiya T, Zhang Y (1996) On the formulation and theory of the Newton interior-point method for nonlinear programming. J Optim Theory Appl 89:507–541
8. Gay DM, Overton ML, Wright MH (1998) A primal-dual interior method for nonconvex nonlinear programming. In: Yuan Y-X (ed) Advances in nonlinear programming. Kluwer Academic Publishers, Dordrecht, pp 31–56
9. Potra FA, Wright SJ (2000) Interior-point methods. J Comput Appl Math 124:281–302
10. Forsgren A, Gill PE, Wright MH (2002) Interior methods for nonlinear optimization. SIAM Rev 44(4):525–597
11. Wright MH (2004) The interior-point revolution in optimization: History, recent developments and lasting consequences. Bull Am Math Soc 42(1):39–56
12. Vanderbei RJ (1999) LOQO: An interior-point code for quadratic programming. Optim Meth & Soft 11–12:451–484
13. Griva I, Shanno DF, Vanderbei RJ, Benson HY (2008) Global convergence analysis of a primal-dual interior-point method for nonlinear programming. Algorithmic Oper Res 3(1):12–19
14. Byrd RH, Hribar ME, Nocedal J (2000) An interior-point algorithm for large-scale nonlinear programming. SIAM J Optim 9(4):877–900
15. Waltz RA, Morales JL, Nocedal J, Orban D (2006) An interior algorithm for nonlinear optimization that combines line search and trust region steps. Math Prog 107(3):391–408
16. Wächter A (2002) An interior point algorithm for large-scale nonlinear optimization with applications in process engineering. PhD thesis, Carnegie Mellon University, Pittsburgh
17. Wächter A, Biegler LT (2005) Line-search filter methods for nonlinear programming: Motivation and global convergence. SIAM J Optim 16(1):1–31
18. Wächter A, Biegler LT (2006) On the implementation of an interior-point filter line-search algorithm for large-scale nonlinear programming. Math Prog 106(1):25–57
19. Benson HY, Shanno DF, Vanderbei RJ (2003) A comparative study of large-scale nonlinear optimization algorithms. In: Di Pillo G, Murli A (eds) High performance algorithms and software for nonlinear optimization. Princeton University, Kluwer Academic Publishers, Princeton, Dordrecht
20. Morales JL, Nocedal J, Waltz RW, Lie G, Goux J-P (2003) Assessing the potential of interior methods for nonlinear optimization. In: Biegler LT, Ghattas O, Heinkenschloss M, van Bloemen Waander B (eds) Large-scale PDE-constrained Optimization, vol 30, Lecture Notes in Computational Science and Engineering, pp 167–183, Springer
21. Nguyen AD, Hachemi A, Weichert D (2008) Application of the interior-point method to shakedown analysis of pavements. Int J Numer Methods Eng 75:414–439
22. Simon J-W, Chen M, Weichert D (2010) Shakedown analysis combined with the problem of heat conduction, vol 2. In: Proceedings of the ASME 2010 Pressure Vessels & Piping Conference, pp 133–142, Bellevue
23. Christiansen E, Andersen KD (1999) Computation of collapse states with von Mises type yield condition. Int J Numer Methods Eng 46(8):1185–1202
24. Andersen ED, Jensen B, Jensen J, Sandvik R, Worsøe U (2009) MOSEK version 6. Technical Report TR–2009–3, MOSEK. URL http://www.mosek.com
25. Trillat M, Pastor J (2005) Limit analysis and Gurson's model. Eur J Mech A/Solids 24:800–819
26. Bisbos CD, Makrodimopoulos A, Pardalos PM (2005) Second-order cone programming approaches to static shakedown analysis in steel plasticity. Optim Meth & Soft 20(1):25–52
27. Makrodimopoulos A (2006) Computational formulation of shakedown analysis as a conic quadratic optimization problem. Mech Res Commun 33:72–83
28. Krabbenhøft K, Lyamin AV, Sloan SW (2007) Formulation and solution of some plasticity problems as conic programs. Int J Solids Struct 44:1533–1549
29. Skordeli M, Bisbos C (2010) Limit and shakedown analysis of 3d steel frames via approximate ellipsoidal yield surfaces. Eng Struct 32(6):1556–1567
30. Sturm JF (1999) Using SeDuMi 1.02. a MATLAB toolbox for optimization over symmetric cones. Optim Meth & Soft 11(12):625–653
31. Tütüncü RH, Toh KC, Todd MJ (2003) Solving semidefinite-quadratic-linear programs using SDPT3. Math Program Ser B 95:189–217
32. Munoz JJ, Bonet J, Huerta A, Peraire J (2009) Upper and lower bounds in limit analysis: Adaptive meshing strategies and discontinuous loading. Int J Numer Methods Eng 77(4):471–501
33. Liu YH, Zhang XF, Cen ZZ (2005) Lower bound shakedown analysis by the symmtric Galerkin boundary element method. Int J Plast 21:21–42
34. Le CV, Gilbert M, Askes H (2009) Limit analysis of plates using the EFG method and second-order conic programming. Int J Numer Methods Eng 78(13):1532–1552
35. Le CV, Nguyen-Xuan H, Askes H, Bordas S, Rabczuk T, Nguyen-Vinh H (2010) A cell-based smoothed finite element method for kinematic limit analysis. Int J Numer Methods Eng 83(12):1651–1674
36. Tran TN, Liu GR, Nguyen-Xuan H, Nguyen-Thoi T (2010) An edge-based smoothed finite element method for primal-dual shakedown analysis of structures. Int J Numer Methods Eng 82:917–938
37. Chen M, Hachemi A, Weichert D (2010) A non-conforming finite element for limit analysis of periodic composites. PAMM Proc Appl Math Mech 10:405–406
38. Ngo N, Tin-Loi F (2007) Shakedown analysis using the p-adaptive finite element method and linear programming. Eng Struct 29(1):46–56
39. Ardito R, Cocchetti G, Maier G (2008) On structural safety assessment by load factor maximization in piecewise linear plasticity. Eur J Mech A/Solids 27:859–881

40. Garcea G, Leonetti L (2009) Numerical methods for the evaluation of the shakedown and limit loads. In: Ambrosio J et al (eds) 7th EUROMECH Solid Mechanics Conference, Lisbon, Portugal
41. Lyamin AV, Sloan SW (2002) Lower bound limit analysis using nonlinear programing. Int J Numer Methods Eng 55:573–611
42. Krabbenhøft K, Damkilde L (2003) A general nonlinear optimization algorithm for lower bound limit analysis. Int J Numer Methods Eng 56:165–184
43. Pastor F, Thoré Ph, Loute E, Pastor J, Trillat M (2008) Convex optimization and limit analysis: application to Gurson and porous Drucker-Prager materials. Eng Fract Mech 75:1367–1383
44. Pastor F, Loute E, Pastor J, Trillat M (2009) Mixed method and convex optimization for limit analysis of homogeneous Gurson materials: a kinematic approach. Eur J Mech A/Solids 28:25–35
45. Pastor F, Loute E (2010) Limit analysis decomposition and finite element mixed method. J Comput Appl Math 234(7):2213–2221
46. Zouain N, Borges L, Silveira J (2002) An algorithm for shakedown analysis with nonlinear yield functions. Comput Methods Appl Mech Eng 191:2463–2481
47. Vu DK, Yan AM, Nguyen-Dang H (2004) A dual form for discretized kinematic formulation in shakedown analysis. Int J Solids Struct 41:267–277
48. Hachemi A, An LTH, Mouhtamid S, Tao PD (2004) Large-scale nonlinear programming and lower bound direct method in engineering applications. In: An LTH, Tao PD (eds) Modelling, Computation and Optimization in Information Systems and Management Sciences. Hermes Science Publishing, London, pp 299–310
49. Hachemi A, Mouhtamid S, Weichert D (2005) Progress in shakedown analysis with applications to composites. Arch Appl Mech 74:762–772
50. Akoa FB, Hachemi A, An LTH, Mouhtamid S, Tao PD (2007) Application of lower bound direct method to engineering structures. J Glob Optim 37(4):609–630
51. Vu DK, Staat M (2007) Analysis of pressure equipment by application of the primal-dual theory of shakedown. Commun Numer Methods Eng 23(3):213–225
52. An LTH, Tao PD (1997) Solving a class of linearly constrained indefinite quadratic problems by DC algorithms. J Glob Optim 11:253–285
53. An LTH, Tao PD (2005) The DC (difference of convex functions) programming and DCA revisited with DC models of real world nonconvex optimization problems. Annals Oper Res 133:23–46
54. Simon J-W, Weichert D (2010) Interior-point method for the computation of shakedown loads for engineering systems. In: ASME Conf Proc ESDA 2010, vol 4, pp. 253–262, Istanbul
55. Simon J-W, Chen M, Weichert D (2011) Shakedown analysis combined with the problem of heat conduction. J Pressure Vessel Technol (in press)
56. Simon J-W, Weichert D (2011) Numerical lower bound shakedown analysis of engineering structures. Comput Methods Appl Mech Eng 200:2828–2839
57. Groß-Weege J (1997) On the numerical assessment of the safety factor of elastic-plastic structures under variable loading. Int. J Mech Sci, 39(4):417–433
58. Vanderbei RJ, Carpenter TJ (1993) Symmetric indefinite systems for interior point methods. Math Prog 58:1–32
59. Kuhn HW, Tucker AW (1950) Nonlinear programming. In: Neyman J (ed) Second Berkeley symposium on mathematical statistics and probability. University of California Press, Berkeley, pp 481–492
60. Nguyen-Thoi T, Vu-Do HC, Rabczuk T, Nguyen-Xuan H (2010) A node-based smoothed finite element method (NS-FEM) for upper bound solution to visco-elastoplastic analyses of solids using triangular and tetrahedral meshes. Comput Methods Appl Mech Eng 199(45–48):3005–3027
61. Belytschko T (1972) Plane stress shakedown analysis by finite elements. Int J Mech Sci 14(9):619–625
62. Corradi L, Zavelani A (1974) A linear programming approach to shakedown analysis of structures. Comput Methods Appl Mech Eng 3:37–53
63. Carvelli V, Cen ZZ, Liu Y, Maier G (1999) Shakedown analysis of defective pressure vessels by a kinematic approach. Arch Appl Mech 69:751–764
64. Schwabe F (2000) Einspieluntersuchungen von Verbundwerkstoffen mit periodischer Mikrostruktur. PhD thesis, Institute of General Mechanics, RWTH Aachen University, Germany
65. Chen HF, Ponter ARS (2001) Shakedown and limit analyses for 3-D structures using the linear matching method. Int J Press Vessels Piping 78:443–451
66. Zhang T, Raad L (2002) An eigen-mode method in kinematic shakedown analysis. Int J Plast, 18:71–90
67. Muscat M, Mackenzie D, Hamilton R (2003) Evaluating shakedown under proportional loading by non-linear static analysis. Comput Struct, 81:1727–1737
68. Garcea G, Armentano G, Petrolo S, Casciaro R (2005) Finite element shakedown analysis of two-dimensional structures. Int J Numer Methods Eng 63:1174–1202
69. Wiechmann K, Stein E (2006) Shape optimization for elasto-plastic deformation. Int J Solids Struct, 43:7145–7165
70. Mouhtamid S (2007) Anwendung direkter Methoden zur industriellen Berechnung von Grenzlasten mechanischer Komponenten. PhD thesis, Institute of General Mechanics, RWTH Aachen University, Germany
71. Chen S, Liu Y, Cen Z (2008) Lower bound shakedown analysis by using the element free Galerkin method and non-linear programming. Comput Methods Appl Mech Eng 197(45-48):3911–3921
72. Krabbenhøft K, Lyamin AV, Sloan SW (2007) Bounds to shakedown loads for a class of deviatoric plasticity models. Comput Mech 39:879–888
73. Zhang G (1992) Einspielen und dessen numerische Behandlung von Flächentragwerken aus ideal plastischem bzw kinematisch verfestigendem Material. PhD thesis, Institut für Mechanik, University Hannover